International Journal of Fracture and Damage Mechanics
Vol. 1: Issue 1
www.journalspub.com

A Comparitive Study on Ceramic Powder Over Static and Dynamic Compaction

M.V. Shanmugam [1], R. Karthikeyan [2], P. Divyakumar[3], R. Nirmal Raja[1]*
[1]Department of Mechanical Engineering, K S R Institute for Engineering and Technology, Tiruchengode, India
[2]Department of Mechanical Engineering, Dr. N.G.P. Institute of Technology, Coimbatore, India
[3]Department of Mechanical Engineering, K S Rangasamy College of Technology, Tiruchengode, India

Abstract

The unique microstructure of dense ceramic powders are studied with the help of both static and dynamic process. Initial density, particle size distribution, particle morphology, and loading path are the various effects that are investigated in the static experiments. At very low velocity steady structured compaction waves are traveling in dynamic experiment. When compared with static response the ceramic powder are found to be significantly stiffer at dynamic response. As deformation is confined to the relatively narrow compaction wave front, density and mechanical properties such as Vickers micro hardness and bending strength of the powder samples were investigated. The increase in impact force tends to decrease springback of the compaction.

****Corresponding Author***
E-mail: karthikeyan.r@drngpit.ac.in

INTRODUCTION

At present there are several developments are undergoing in industries by changing the materials in order to improve in both mechanical and physical properties. In such cases, ceramics are been replaced for various different materials and even several matrix composites are used. Combination of compaction and sintering are taking place for ceramic parts. Basically cracks are originated during the compaction process in powder metallurgy (P/M). But the cracks will not be visible until the sintering process is done. Since only after the sintering process there will takes place some changes in boundary conditions and micro structure. The root cause is most likely the poor inter-particle bonding obtained prior to the sintering. The compaction of ceramic powders using both static and dynamic processes has been extensively studied from the standpoint of the manufacture of nearly fully dense ceramics with unique microstructures from precursor ceramic powders. In these investigations, the change in properties can be determined by the pressure applied during the compaction and also depends on the temperature during the sintering process. Besides manufacturing issues, the behaviour of ceramic powders under dynamic loading is important for understanding the behaviour of geological materials for seismic coupling, penetration, and planetary science applications, as well as the performance of ceramic armour.

Ceramic Powder

Basically in powder metallurgy, the powders have to be fine grained. Similarly the ceramic powder characteristic and process which includes compaction and sintering are to be decided before the start of operation. If not there may produce a strong impact over mechanical behaviour of the parts that may produce some defects (i.e.) pores, micro cracks, density gradient and agglomerates) In particular, the mechanical characteristics of the solid obtained after cold forming may affect the sintering process and thus the mechanical properties of the final piece.

Compaction

Uniaxial die compaction is the simplest form of consolidation process that has been extensively used to density powder materials. One disadvantage of this technique, however, is the variation of the pressed density that can occur at different locations of the parts. Dynamic compaction methods differ from the conventional consolidation methods in respect of the compacting pressure and the speed or rate of compaction used (Clyns, 1977). This work provides some evidence to suggest that increasing the rate of compaction results in a more uniform density distribution, improved green strength and in the case of die compaction, lower compact ejection forces.

Shock – Wave Propagation

The sharp shock-front, and the pressure relaxation period (rarefaction) are the two important factor in ideal shock-wave profile. A part of the shock-wave, which is preceded of the whole stress pulse, is an elastic wave characterised by an intensity equal to the elastic limit of the material. Hugoniot Elastic Limit (HEL) can be described that the elastic limit under the imposed stress and strain rate conditions is reached. The pulse duration depends on the time required for the wave to travel through the material (Figure 1).

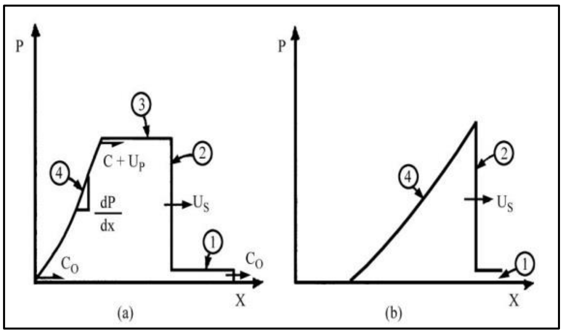

Fig. 1. *The Ideal Shock-Wave Profile Formed by: (a) High-Speed Impact of a Projectile to a Target; (b) the Detonation of an Explosive Substance in Contact to Thematerial or by Pulsed Laser Radiation.*

The shock-waves, formed by the high-speed impact of a projectile to a target, has a trapezoidal form, whereas those formed by the detonation of an explosive substance or by pulsed laser radiation has the triangular form. A real shock-wave profile (P-t), determined by laser interferometry. Beyond the HEL, the pressure rises continuously to the top and the rate of rise is dictated by the constitutive behaviour of the material. At the top of the curve there is the pulse duration, which is followed by the unloading curve.

Dynamic compaction is an alternative way to consolidate plastic, ceramic, and metallic powders and combinations. Powders have been modified by shock wave propagation in order to increase their reactivity or sinterability. The principle behind the shock modification of powders is the generation of a high concentration of defects in the lattice, by the propagating shock wave. The high pressures and strain rates that occur in dynamic compaction of powders can result in phase transformation of the material.

LITERATURE REVIEWED ON THE COMPACTION BASED ON MATERIAL

Faraz Khan et al. [1] registered that High Velocity Compaction (HVC) technique is been used in compaction of Ti–6Al–4V. High velocity compaction technique was applied to the compaction of pre-alloyed, hydride–dehydride Ti–6Al–4V powder. The powder was pressed in single stroke with a compaction speed of 7.10– 8.70 ms_1. The green samples were sintered at 1300°C in Ar-gas atmosphere. Scanning electron microscope (SEM) was used to examine the surface of the sintered samples. Density and mechanical properties such as Vickers micro hardness and bending strength of the powder samples were investigated. The sintered compacts exhibited a maximum relative density of 99.88% with a sintered density of 4.415 g cm_3, hardness of 364–483 HV and the bending strength in the range of 103–126.78 MPa. The Impact force strongly affects the green and sintered density of compacts.

Khoei et al. [2] registered the dynamic modeling of powder compaction processes is presented based on a simple contact algorithm to evaluate the distribution of final density in dynamic powder die-pressing. The large deformation frictional contact is employed by imposing the contact constraints via the contact node-to-surface formulation and modifying the contact properties of frictional slip. The Coulomb friction law is used to simulate the friction between the rigid punch and the work-piece.

Grady et al. [3] registered that Shear deformation is enhanced when the material subject to shock compression is in an initial distended state. Shock Hugoniot data for full-density and porous compounds of boron carbide, silicon dioxide, tantalum pentoxide, uranium dioxide and playa alluvium are investigated for purposes of equation-of-state representation of intense shock compression. Hugoniot data of distended materials reveal evidence of accelerated solidesolid phase transition as a consequence of shock compaction and accompanying enhanced shear deformation.

Hazell et al. [4] registered that the ballistic compaction and penetration of ceramic powder targets has been studied experimentally and computationally using powder compacts of different initial densities and thickness. Using a non-deforming conically-nosed projectile, confined alumina powder compacts have been penetrated at velocities of ~375 m/s and ~900 m/s. For compacts where the initial density increases linearly for a decreasing thickness, both experimental and computational results show that there is very little difference in the resistance to projectile penetration. Furthermore, it was shown that increasing the density of the compact for a given thickness was shown to have more of an effect on ballistic resistance than increasing the thickness for a given density.

Gu et al. [5] registered that the continuous recording of the stress profiles in ceramic powders subject to shock loading with manganin gauges. A series of plate impact experiments on highly porous ceramic powders such as Al2O3, SiC and B4C were conducted at the laboratory’s single stage powder gun facility. The relationship between shock wave velocity and particle velocity was measured to obtain the Hugoniot data. Plate impact onto powder sample experiments were conducted at loading stresses ranging from 1.6 to 4.2 GPa. Hopkinson bar dynamic compression test results and powder gun plate impact experiment results. The P–V diagram shows that the crush strength of ceramic powders is comparable to the loading stress level.

Borg et al. [6] registered to apply and compare different computational compaction models to the dynamic compaction of porous silicon dioxide (SiO_2) powder. Two hydrodynamic codes, KO and CTH, were used to simulate the experimental results. Two compaction models, P–a and P–l were implemented within CTH in conjunction with the MieGruneisen (MG) equation of state. The snow plow (SP) compaction model was implemented within KO. Two hydrodynamic codes, KO and CTH, were used to simulate the experimental results. Two compaction models, P–a and P–l were implemented within CTH in conjunction with the MieGruneisen (MG) equation of state.

MATHEMATICAL MODELING

Spring Back and Peak Load

The axial force at the top of the punch, F_{top}, was measured by the load cell of the testing machine. Accounting for the frictional forces that developed during the USC tests, the axial stress, r, applied to the specimen was approximated as Eq. (1).[7]

$$\sigma = \frac{F_{top} - F_{frict}}{A_0} \tag{1}$$

Spring back of the green compacts was calculated using the general formula as shown in Eq. (2)

$$\delta = \frac{l - l_0}{l_0} \tag{2}$$

The resultant peak load was converted into the bending strength based on the following Eq. (3).

$$S = \frac{3 \times P \times L}{2 \times t^2 \times W} \tag{3}$$

where S is the bending strength of compact, P is rupture force, L is the span of the clamp, t is the height of compact, W is the width of compact.

Specimen Volume

Changes in specimen volume, ΔV, were calculated assuming uniaxial strain conditions. Axial deformation was measured by the LVDT on the test fixture. This LVDT tracked the displacement of the upper punch relative to lower punch, so the displacement measurements included deformations of both the specimen and the non-specimen components (e.g., upper and lower punches, interface closure, etc.) within the gage length. The non-specimen component of the displacement, system, was quantified by loading a calibration specimen fabricated from a standard material (aluminium) and subtracted from the measured displacement during data reduction. [8–12]

The change in specimen volume was then calculated from:

$$\Delta V = A_0\,(\delta_{specimen}) = A_0\,(\delta_{total} - \delta_{system}) \tag{4}$$

The Hugoniot state for the powder is constrained to lie on this release path and along a Rayleigh line from the origin with slope given by

$$\rho_{00} U_s = \frac{\Delta\sigma}{\Delta U_p} \tag{5}$$

From these uncertainties, the uncertainty in the shock velocity is estimated using the first order uncertainty expression (Coleman and Steele, 1989) for random errors

$$\delta U_s = \sum_{i=0}^{N} \left(\left(\frac{\partial U_s \delta x_i}{\partial x_i} \right)^2 + \left(\frac{\partial U_s}{\partial t_i} \delta t_i \right)^2 \right)^{\frac{1}{2}} \tag{6}$$

The plastic hardening/softening modulus and flow direction vector are defined as:

$$H = -\left(\frac{\partial F}{\partial K}\right)\left(\frac{\partial K}{\partial \varepsilon}\right)^T n_Q \tag{7}$$

$$\frac{\partial F}{\partial \sigma} = C_1 \frac{\partial J_1}{\partial \sigma} + C_2 \frac{\partial (J_{2D})^{1/2}}{\partial \sigma} + C_3 \frac{\partial J_{3D}}{\partial \sigma} \tag{8}$$

Hardening Coefficient

The evolution of yield surface depends on the hardening coefficient where the yield surface expands or shrinks from its original position. The void ratio change by an elastic component can be written as

$$\Delta e^{e} = \mathrm{K}\ln\left(\frac{\sigma_{\mathrm{A}}}{\sigma_{\mathrm{A}_0}}\right) \tag{9}$$

And the plastic component as

$$\Delta e^{p} = -(\lambda - \mathrm{k})\ln\left(\frac{\sigma_{\mathrm{A}}}{\sigma_{\mathrm{A}_0}}\right) \tag{10}$$

Equilibrium equation can be derived in a general form as shown

$$\left(\frac{\partial \sigma_{zz}}{\partial Z}\right) + \frac{1}{r}\frac{\partial \sigma_{\theta z}}{\partial \theta} + \frac{\partial \sigma_{rz}}{\partial r} + \frac{\sigma_{rz}}{r} = 0 \tag{11}$$

Here axial symmetry will be assumed where the cylinder will maintain its form and by excluding torsion, $\sigma_{\theta z} = \sigma_{r\theta.}$ is substituted in Eq. (11).

$$\frac{\partial \sigma_{zz}}{\partial z} + \frac{\partial \sigma_{rz}}{\partial r} + \frac{\sigma_{rz}}{r} = 0 \qquad (12)$$

The reduced equilibrium equation is

$$\pi r2(\sigma_z + d\sigma_z) - \pi r^2\sigma_z + 2\pi\mu r\sigma_r dz = 0 \qquad (13)$$

where σ_z is the axial stress at distance z from the surface, σ_r the radial stress and μ the coefficient of friction between the container wall and the compact powder.

A simplification of above equation yields

$$d\sigma_z = -\frac{2\mu\sigma_r dz}{r} \qquad (14)$$

$$\sigma_r = \sigma_z + \bar{\sigma} \qquad (15)$$

$$\frac{d\sigma_z}{\sigma_{z+\bar{\sigma}}} = -\frac{2\mu}{r}dz \qquad (16)$$

The final expression for the instantaneous axial stress as a function of the compaction process parameters is given by:

$$\frac{\sigma_z}{\bar{\sigma}} = \left[1 + \frac{p_a}{\bar{\sigma}}\right]\left[exp\left\{\frac{\mu(H-2Z)}{r}\right\}\right] - 1 \qquad (17)$$

CONCLUSION

The Impact force strongly affects the green and sintered density of compacts. As impact force arises, both the green density and the sintered one increases gradually. Relative density of the sintered compacts pressed at impact force 1.857 kN reaches up to 99.88%. With increasing impact force, the bending strength and the Vickers hardness of the sintered samples increase gradually. The spring back of the green compacts decreases gradually with increasing impact force.

FUTURE SCOPE

By applying a constant impact force during compaction there will be a steady shock wave. In order to improve the mechanical properties, a perfect binder have to be added. Increase in green density and mechanical properties with increasing impact force and also making a good combination of sintering temperature and holding time

REFERENCE

1. Faraz Khan D., Yin H., Li H., *et al. Compaction of Ti–6Al–4V Powder Using High Velocity Compaction Technique.* Elsevier, Materials and Design 50; 2013, 479–83p.
2. Li H., Yin H., Faraz Khan D., *et al. High Velocity Compaction of 0.9Al2O3/Cu Composite Powder*. Elsevier, Materials and Design 57; 2014, 546–50p.
3. Vogler T.J., Lee M.Y., Grady D.E. Static and dynamic compaction of ceramic powders, *Int J Solids Struct.* 2007; 44: 636–58p.
4. Khoei A.R., Biabanaki S.O.R., Parvaneh S.M. Dynamic modeling of powder compaction processes via a simple contact algorithm, *Int J Mech Sci.* 2012; 64: 196–210p.
5. Grady D., Fenton G., Vogler T. Equation of state and evidence of enhanced phase transformation for shock compression of distended compounds, *Int J Impact Eng.* 2013; 56: 19–26p.
6. Zohoor M., Mehdipoor A. Explosive compaction of tungsten powder using a converging underwater shock wave, *J Mater Process Technol.* 2009; 209: 4201–6p.
7. Khoei A.R., Biabanaki S.O.R., Parvaneh S.M. 3D dynamic modeling of powder forming processes via a simple and efficient node-to-surface contact algorithm, *Appl Math Model.* 2013; 37: 443–62p.
8. Hazell P.J., *et al.* Ballistic compaction of a confined ceramic powder by a non-deforming projectile: experiments

and simulations, *Mater Des*. 2014; 56: 943–52p.
9. Rahman M.M., Appleby-Thomas G.J., Toone S. Development of a finite element model of metal powder compaction process at elevated temperature, *Appl Math Model*. 2009; 33: 4031–48p.
10. Gu Y.B., Ravichandran G. Dynamic behavior of selected ceramic powders, *Int J Impact Eng*. 2006; 32: 1768–85p.
11. Al-Qureshi H.A., Galiotto A., Klein A.N. On the mechanics of cold die compaction for powder metallurgy, *J Mater Process Technol*. 2005; 166: 135–43p.
12. Buchheit T.E. Measurement of ceramic powders using instrumented indentation and correlation with their dynamic response, *Mech Mater*. 2010; 42: 599–614p.